DOI: 10.1002/chem.200900864

Highly Emissive Diborylphenylene-Containing Bis(phenylethynyl)benzenes: Structure–Photophysical Property Correlations and Fluoride Ion Sensing

Cui-Hua Zhao, Eri Sakuda, Atsushi Wakamiya, and Shigehiro Yamaguchi*[a]

Abstract: A series of 2,5-bis(dimesitylboryl)-1,4-bis(arylethynyl)benzenes **1**–**6** that contain various *p*-substituents on the terminal benzene rings, including NPh_2 (**1**), OMe (**2**), Me (**3**), H (**4**), CF_3 (**5**), and CN (**6**) groups, were synthesized, and the effects of the *p*-substituents on the absorption and fluorescence properties were investigated both in solution and in the solid state. Linear relationships were obtained not only between the Hammett σ_p^+ constants of the *p*-substituents and the absorption and fluorescence maxima, quantum yields, and excited-state dynamics parameters in solution, but also between the σ_p^+ constants and the fluorescence quantum yields in the solid state. An important finding extracted from these results is that the suppressed fluorescence quenching in the solid state is a common feature for the present laterally boryl-substituted π-conjugated skeletons. Hence, the diborylphenylene can serve as a useful core unit to develop highly emissive organic solids. In fact, most of the derivatives showed more intense emission in the solid state than in solution. In addition to these studies, the titration experiment of **1** by the addition of nBu$_4$NF was conducted, which showed the stepwise bindings of two fluoride ions with high association constants as well as a drastic change in the fluorescence spectra, while constantly maintaining high quantum yields (0.61–0.76), irrespective of the binding modes. This result also demonstrated the potential utility of the present molecules as an efficient fluorescent fluoride ion sensor.

Keywords: boron · fluorescence · fluoride ion sensor · structure–property relationships · substituent effects

Introduction

Tri-coordinate boron-containing π-conjugated systems have attracted considerable attention due to their intriguing electronic and photophysical properties, which arise from the p_π–π* conjugation between the vacant p orbital on the boron atom and the π* orbital of the π-conjugated framework.[1] The compounds classified into this category have been utilized in a wide range of fields, including nonlinear optics,[2,3] two-photon absorption and emission materials,[4,5] organic light-emitting diodes (OLEDs),[6–9] and chemical sensors for fluoride ions.[10–15] Most of the reported organoboron materials typically either contain the boron atoms in the main chain or bear the boryl groups at the terminal positions of the π-conjugated framework. In contrast, we and other research groups recently reported the introduction of the boryl groups at the lateral positions of the π-conjugated framework as a new design of the boron-based materials.[16–18] In particular, we reported that the incorporation of the boryl groups on the electron-donating π-conjugated skeleton, such as bis[(*p*-Ph_2N-phenyl)ethynyl]benzene (**1**), is an efficient way to create emissive organic solids.[16a] This design has a certain generality. Thus, we also demonstrated that boryl-substituted oligothiophenes showed intense solid-state emissions, the color of which could be easily tuned in a full-color region from blue to red by appropriate structural modification.[16c] Similar boryl-substituted polythiophenes were also independently synthesized by Jäkle and co-workers.[17]

The design and synthesis of highly emissive organic solids is a fundamental subject for various photonic and optoelectronic applications. Although a number of emissive fluorophores with a fluorescence quantum yield of near unity in solution exist, the examples of highly emissive organic solids are still limited, because of the severe fluorescence quenching as a result of certain intermolecular interactions.[19]

[a] Dr. C.-H. Zhao, Dr. E. Sakuda, Dr. A. Wakamiya, Prof. Dr. S. Yamaguchi
Department of Chemistry, Graduate School of Science
Nagoya University, Furo, Chikusa, Nagoya 464-8602 (Japan)
Fax: (+81) 52-789-5947
E-mail: yamaguchi.shigehiro@b.mbox.nagoya-u.ac.jp

Supporting information for this article is available on the WWW under http://dx.doi.org/10.1002/chem.200900864.

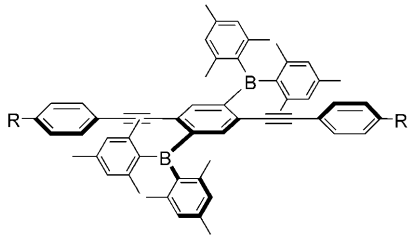

1: R = NPh_2 **2**: R = OMe
3: R = Me **4**: R = H
5: R = CF_3 **6**: R = CN

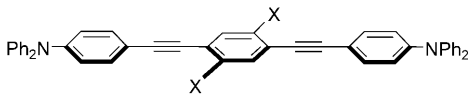

7: X = Si(*i*Pr)$_3$
8: X = CN

Therefore, the rational design of such emissive organic solids is still a challenging issue.[20] In this regard, the elucidation of the structure–property relationship of the known highly emissive systems should provide an important basis for further rational designs. On the basis of this motivation, we herein investigate the structure–property correlations in a series of bis[(*p*-substituted phenyl)ethynyl]diborylbenzenes **1**–**6**, including the already reported *p*-Ph_2N-substituted derivative **1**.

In the previous study on **1**, we learned some important issues about the effect of the lateral dimesitylboryl groups, through comparisons of **1** with other analogous compounds that contain bulky triisopropylsilyl groups (**7**) or electron-withdrawing cyano groups (**8**), instead of the boryl groups. Among these compounds, only **1** can maintain an intense emission in the solid state. These facts demonstrated that there are two crucial requirements for achieving an intense solid-state emission. One is steric bulkiness that can prevent an intermolecular interaction. The other is a π-electron-accepting character that leads to an intramolecular charge-transfer (CT) transition with a large Stokes shift, which should effectively suppress self-quenching in the condensed phase. Notably, the lateral dimesitylboryl groups in **1** can satisfy these two requirements.

To elucidate the more detailed structure–property correlation, we herein focused our attention on the substituent effects of the terminal phenyl rings. We prepared a series of bis(arylethynyl)benzene derivatives **1**–**6** that contain electron-donating Ph_2N (**1**) and MeO (**2**) groups, electronically indifferent Me (**3**) and H (**4**) groups, and electron-withdrawing CF_3 (**5**) and CN (**6**) groups as the *p*-substituents and comprehensively studied their photophysical properties, including the excited-state dynamics and solid-state fluorescence. We also studied their application to a fluorescent chemosensor for fluoride ions, to demonstrate the utility of these highly emissive fluorescent molecular systems.

Results and Discussion

Synthesis: In the previous work, the synthetic route to the boryl-substituted bis(arylethynyl)benzene **1** was established based on the Pd^0/CuI-catalyzed Sonogashira reaction with 1,4-diethynyl-2,5-bis(dimesitylboryl)benzene (**9**) as a key precursor.[16a] This facile synthetic route allowed us to prepare a series of the derivatives **2**–**6** containing various terminal substituents by using appropriate *p*-substituted phenyl iodides, as shown in Scheme 1. The coupling reaction of

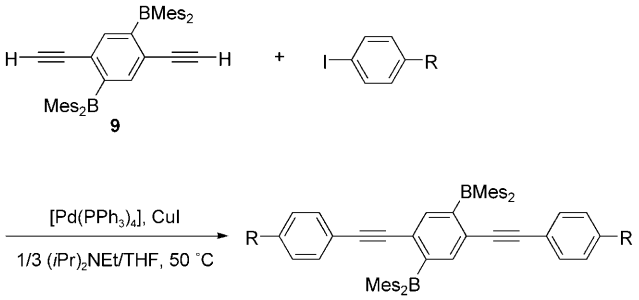

1: R = NPh_2 (59%)
2: R = OMe (53%)
3: R = Me (44%)
4: R = H (72%)
5: R = CF_3 (84%)
6: R = CN (93%)

Scheme 1. Synthesis of bis[(*p*-substituted phenyl)ethynyl]diborylbenzenes **1**–**6**.

phenyl iodides that contain electron-withdrawing *p*-substituents, such as CF_3 and CN proceeded in higher yields than with those that contain electron-donating groups, such as OMe and NPh_2, probably because the electron-donating groups on the aryl halides generally have a detrimental effect on the coupling reaction.[16b,21] All the obtained boryl-substituted π-conjugated compounds are stable in air and water and can be purified by silica-gel column chromatography.

X-ray crystal structure analysis: Among the newly prepared bis(arylethynyl)benzenes, the structures of nonsubstituted **4** and cyano-substituted **6** were determined by X-ray crystallography. Their ORTEP drawings are shown in Figure 1. The structure of Ph_2N-substituted **1** was reported in the previous paper.[16a] In all these three compounds, the trivalent boron centers are well protected by the methyl groups at the *o*-positions of two mesityl groups, which accounts for their high stabilities. It is worth noting that the *p*-substituents at the terminal phenyl rings of the bis(arylethynyl)benzene skeleton seem to have a certain influence on the coplanarity of the π-conjugated framework. Thus, while Ph_2N-substituted **1** has a significantly twisted main chain structure, in which the dihedral angle between the central and terminal benzene rings is 47.5°, nonsubstituted **4** has a slightly decreased dihedral angle of 37.4°, and compound **6**, which contains strong electron-withdrawing CN groups, adopts an

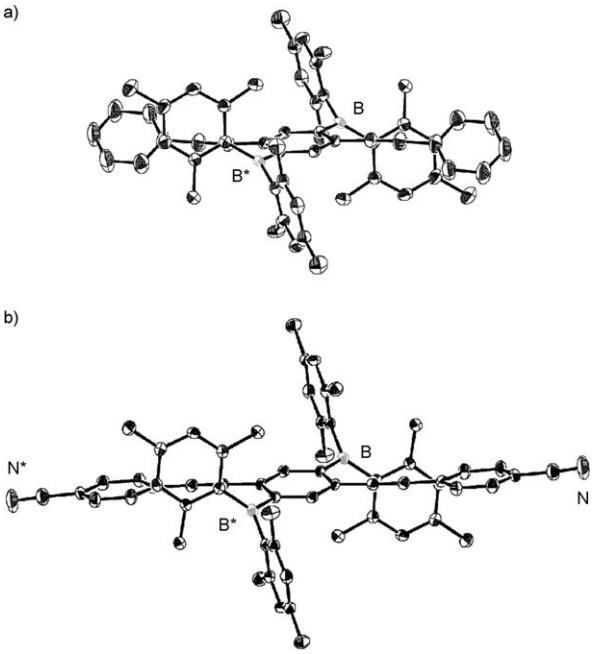

Figure 1. ORTEP drawings of a) **4** and b) **6**. Thermal ellipsoids are drawn at the 50% probability level. Hydrogen atoms are omitted for clarity.

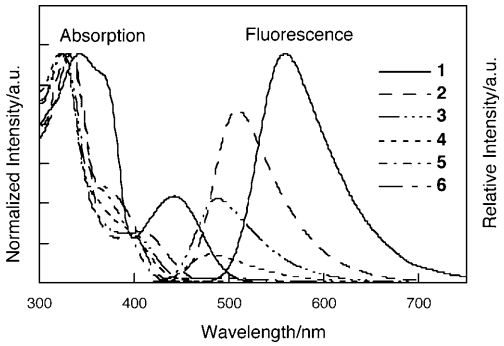

Figure 2. Absorption and fluorescence spectra of boryl-substituted bis(arylethynyl)benezenes **1**–**6** in benzene.

Table 1. UV/Vis absorption and fluorescence data for boryl-substituted bis(arylethynyl)benezenes **1**–**6** in benzene.

	Absorption[a]	Fluorescence			Excited-state dynamics	
	λ_{abs} [nm] (log ε)	λ_{em} [nm][b]	Φ_F[c]	τ_s [ns]	k_r [s^{-1}]	k_{nr} [s^{-1}]
1	442 (4.37)	559	0.98	5.4	1.8×10^8	3.7×10^6
2	409 (4.05)	509	0.74	7.5	9.8×10^7	3.4×10^7
3	401 (4.09)[d]	487	0.36	4.6	7.8×10^7	1.4×10^8
4	400 (3.96)[d]	480	0.16	3.2	5.1×10^7	2.7×10^8
5	368 (4.27)[d]	476	0.04	1.9	2.1×10^7	5.1×10^8
6	377 (4.34)[d]	476	0.04	1.5	2.7×10^7	6.6×10^8

[a] Only the longest absorption maximum wavelengths are given. [b] Excited at the longest absorption maximum. [c] Absolute quantum yield determined by a calibrated integrating sphere system. [d] Observed as shoulder.

almost coplanar main chain structure with a dihedral angle of only 9.8°. Although we cannot rule out the packing effect on the coplanarity of the π-conjugated skeleton at this stage, these differences suggest that the π conjugation occurs more effectively as more electron-withdrawing groups are attached at the terminal positions. On the contrary, as for the geometry of the boron moieties, the dihedral angles between the central benzene ring and the boron planes are 44.68° for **6**, 36.64° for **4**, and 39.37° for **1**. Thus, no significant correlation was observed between the electronic nature of the terminal *p*-substituents and the effectiveness of the p_π–π* conjugation in the central diborylbenzene moiety.

Photophysical properties: To elucidate the effect of the terminal substituents on the photophysical properties for the boryl-substituted bis(arylethynyl)benzenes **1**–**6**, we investigated the following three issues: Effects of the *p*-substituents on 1) the photophysical properties in solution, 2) the excited-state character and the delocalization of molecular orbitals, and 3) the solid-state fluorescence properties.

Photophysical properties in benzene solutions: The UV/Vis absorption and emission spectra of compounds **1**–**6** in benzene are shown in Figure 2, the data for which are summarized in Table 1. All these derivatives have an intense absorption band at ca. 320–340 nm and a weaker band at longer wavelengths of 368–442 nm. While the former band is assignable to the π–π* transition of the bis(arylethynyl)benzene skeleton, the latter band is assigned to the intramolecular charge-transfer (CT) transition from the HOMO delocalized over the whole π-conjugated framework to the LUMO mainly localized on the diborylphenylene moiety. The latter band shifts to longer wavelengths as the electron-donating ability of the *p*-substituent increases from **6** (377 nm) to **1** (442 nm).

In the fluorescence spectra, the emission properties of the bis(arylethynyl)benzenes are highly dependent on the electronic nature of the terminal *p*-substituents. Similar to the trend in the longer wavelength band in the absorption spectra, the emission maximum wavelength is red-shifted with the increase in the electron-donating ability of the terminal *p*-substituents, from a greenish/blue fluorescence at 476 nm for **6** to a yellow emission at 559 nm for **1**. In conjunction with this change, the fluorescence intensity also increases with the increased electron-donating ability of the terminal *p*-substituents.

We correlated these photophysical data with the Hammett substituent constants σ_P^+.[22] We found that not only the absorption maxima, but also the emission maxima have linear relationships with the σ_P^+ parameters of the *p*-substituents. According to the plots in Figure 3, the relationships shown in Equations (1) and (2) can be derived, although the correlation value *r* in the latter case is moderate. These results may be rationalized by considering that the absorption and emission maxima of the present systems are highly dependent on their HOMO energy levels. As the σ_P^+ value de-

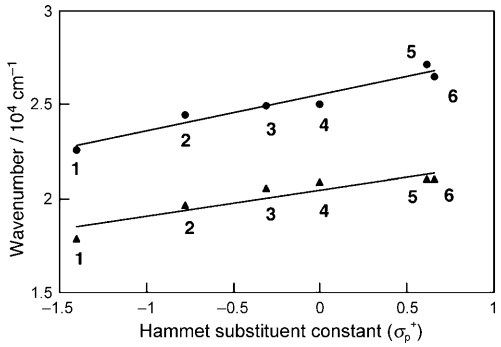

Figure 3. Correlations between the absorption (●) and emission (▲) maxima and the Hammett substituent constants (σ_p^+) of the terminal substituents in the boryl-substituted bis(arylethynyl)benzenes **1**–**6**.

creases, the HOMO energy levels increase, leading to the intramolecular CT transition at the longer wavelength.

$$\nu_{abs}\ [cm^{-1}] = 1939\sigma_p^+ + 25\,513\ (r = 0.969) \quad (1)$$

$$\nu_{em}\ [cm^{-1}] = 1406\sigma_p^+ + 20\,439\ (r = 0.924) \quad (2)$$

It is worth noting that the fluorescence quantum yields also have a linear relationship with the Hammett parameters. Figure 4 shows the plot of the quantum yields (Φ_F) of

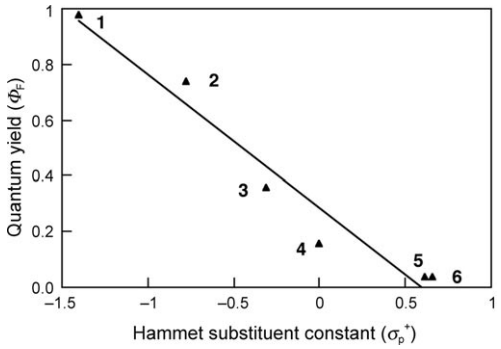

Figure 4. Correlation between the fluorescence quantum yield (Φ_F) in benzene and the Hammett constant (σ_p^+) of the terminal substituents in the boryl-substituted bis(arylethynyl)benzenes **1**–**6**.

1–**6** against the Hammett σ_P^+ constants, which gives Equation (3). Although electron-withdrawing CN-substituted **6** shows only a weak fluorescence ($\Phi_F = 0.04$), the electron-donating Ph_2N-substituted **1** exhibits a very intense emission with a Φ_F of 0.98, even though it has a highly twisted main chain structure.

$$\Phi_F = -0.477\sigma_p^+ + 0.289\ (r = 0.977) \quad (3)$$

To elucidate the structure–property correlation in more detail, we also determined the fluorescence lifetime (τ_s) by a time-resolved photoluminescence study and calculated the radiative (k_r) and nonradiative (k_{nr}) decay rate constants from the singlet excited state, based on the equations $\Phi_F = k_r \times \tau_s$ and $k_r + k_{nr} = \tau_s^{-1}$. According to the calculated k_r and k_{nr} values, the replacement of the terminal NPh_2 groups with less electron-donating or -withdrawing groups leads to acceleration of the nonradiative process and deceleration of the radiative process at the same time. The linear relationships were observed between not only k_r and σ_P^+, but also k_{nr} and σ_P^+, as shown in Figure 5, from which Equations (4) and (5)

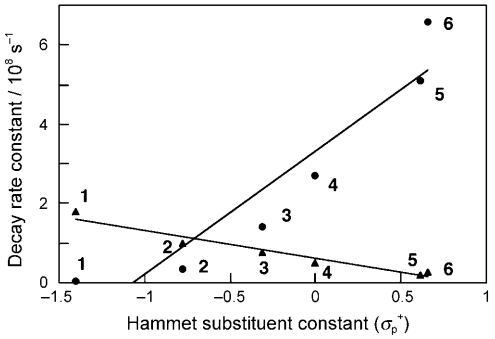

Figure 5. Correlations between the radiative (k_r, ▲) and nonradiative (k_{nr}, ●) decay rate constants and the Hammett substituent constants (σ_p^+) of the terminal substituents in the boryl-substituted bis(arylethynyl)benzenes **1**–**6**.

were obtained, although in the latter case the correlation value was only moderate. Importantly, the steeper slope in Equation (5) compared to that in (4) implies that the difference in k_{nr} predominantly contributes to the significant change in the fluorescence efficiency. These results demonstrate that the electron-donating terminal groups are essential for realizing the intense fluorescence in the present boryl-substituted π-conjugated systems.

$$k_r\ [s^{-1}] = -0.712 \times 10^8\sigma_p^+ + 0.614 \times 10^8\ (r = 0.970) \quad (4)$$

$$k_{nr}\ [s^{-1}] = 3.10 \times 10^8\sigma_p^+ + 3.32 \times 10^8\ (r = 0.937) \quad (5)$$

Fluorescence solvatochromism and theoretical studies: The most notable feature of the present boryl-substituted bis(aryl-ethynyl)benzenes is their intramolecular CT character in the transitions. To gain a deeper insight into their excited states, we investigated the solvent effects in the absorption and fluorescence spectra for the representative derivatives, electron-donating Ph_2N-substituted **1**, nonsubstituted **4**, and electron-withdrawing CN-substituted **6**, the data for which are summarized in Table 2.

In all these compounds, while the absorption maxima show only trivial solvent dependence, the fluorescence spectra show substantial bathochromic shifts as the solvent polarity increases. These facts demonstrate that these molecules have more polar structures in the excited state relative to those in the ground state, similar to other boryl-substituted π-conjugated compounds. To compare the degree of the polar excited-state structure among these molecules, we employed the Lippert–Mataga equation [Eq. (6)].

Table 2. UV/Vis absorption and fluorescence data of boryl-substituted bis(arylethynyl)benzenes **1**, **4**, and **6** in various solvents.

	Solvents	λ_{abs} [nm][a]	λ_{em} [nm][b]	$\Delta\nu$ [cm^{-1}][c]
1	cyclohexane	432	536	4491
	benzene	442	559	4753
	$CHCl_3$	438	567	5194
	THF	437	601	6244
	MeOH	439	627	6830
4	cyclohexane	400[d]	474	3902
	benzene	400[d]	480	4167
	$CHCl_3$	398[d]	489	4676
	THF	396[d]	488	4760
	MeOH	397[d]	496	5027
6	cyclohexane	370[d]	460	5287
	benzene	377[d]	476	5516
	$CHCl_3$	366[d]	484	6661
	THF	368[d]	504	7332

[a] Only the longest absorption maximum wavelengths are given. [b] Excited at the longest absorption maximum. [c] Stokes shift. [d] Observed as shoulder.

$$\Delta\nu = \frac{2\Delta f}{hca^3}(\mu_e - \mu_g)^2 + C \quad (6)$$

$$\Delta f = \frac{\varepsilon - 1}{2\varepsilon + 1} - \frac{(n^2-1)}{(2n^2+1)} \quad (7)$$

in which C is a constant, μ_e and μ_g are the dipole moments in the excited state and ground state, respectively, and $\Delta\nu$ is the Stokes shift. Δf is the solvent polarity and is given by Equation (7) in which ε is the dielectric constant and n is the optional refractive constant. Although this equation originally assumes the presence of a molecular dipole, it has been demonstrated to be applicable to several quadrupole extended π-conjugated molecules.[23] For the present compounds **1**, **4**, and **6**, we indeed obtained linear relationships for the plots of $\Delta\nu$ as a function of the Δf, as shown in Figure 6. The slopes obtained for compounds **1** and **6** are 7213 and 8974 cm^{-1}, respectively, which are comparable to each other and much steeper than that of **4** (3327 cm^{-1}). These results indicate that the quadrupole moments in the excited state are significant not only in **1** but also in **6**. While it is reasonable that the electron-donating Ph_2N-substituted **1** has such a large quadrupole moment in the excited state, the steep slope obtained for CN-substituted **6** is beyond our expectation. The large quadrupole moment in the excited state would cause a significant structural relaxation, which may be one of the factors for the larger k_{nr} value for **6**. However, this explanation is not applicable to the rationalization of the small k_{nr} value of Ph_2N-substituted **1**. Therefore, the discussion of the difference in the k_{nr} values for these compounds may need a more careful consideration taking the intersystem crossing process into account.

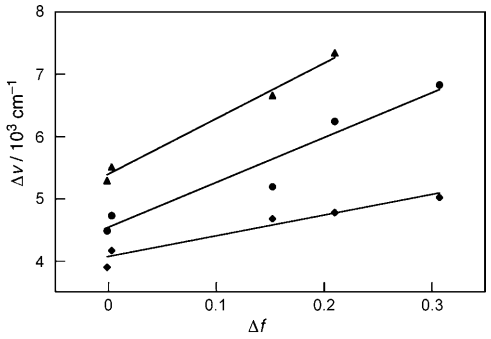

Figure 6. The Lippert–Mataga plots for boryl-substituted bis(arylethynyl)-benzenes **1** (●), **4** (◆), and **6** (▲).

To elucidate the effect of the terminal *p*-substituents on the electronic structures, we conducted single-point calculations of the three compounds **1**, **4**, and **6** at the B3LYP/6-31G(d) level of theory, by using the geometries derived from their crystal structures. We also performed time-dependent density-functional theory (TD-DFT) calculations of these three compounds at the B3LYP/6-31G(d) level of theory to understand their intramolecular CT transitions. The pictorial drawings of their molecular orbitals are shown in Figure 7, and the calculated data are summarized in Table 3.

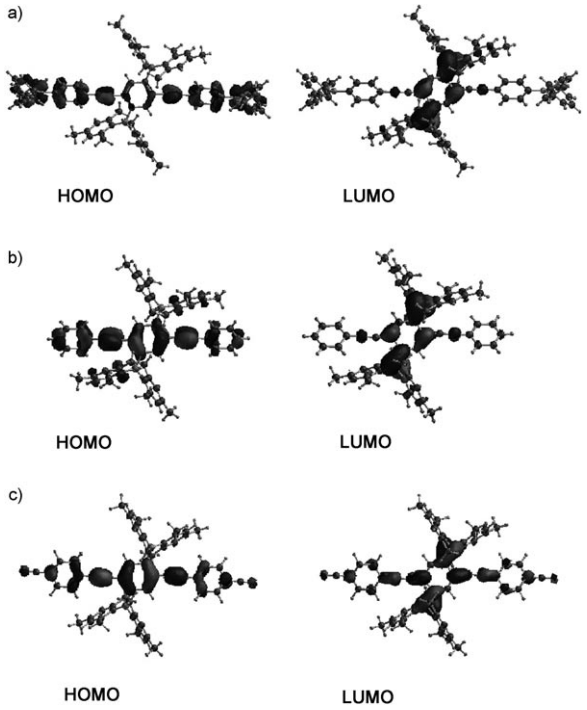

Figure 7. Pictorial drawings of the HOMO and LUMO for a) **1**, b) **4**, and c) **6**, calculated at the B3LYP/6-31G(d) level of theory by using their crystal structures.

Table 3. Calculated Kohn–Sham molecular orbital energy levels and the first excited-state energies for the boryl-substituted bis(arylethynyl)benzenes **1**, **4**, and **6**.

	HOMO [eV]	LUMO [eV]	HOMO–LUMO gap [eV]	Transition energy[a] [eV] (λ [nm])	f[b]
1	−4.74	−1.86	2.88	2.28 (545)	0.574
4	−5.36	−1.95	3.41	2.86 (434)	0.0972
6	−5.84	−2.63	3.21	2.81 (442)	0.552

[a] The first excited-state transition energy. [b] Oscillator strength.

The nonsubstituted compound **4** has a HOMO delocalized over the whole bis(arylethynyl)benzene framework, whereas its LUMO is mostly localized on the central diborylphenylene moiety. The HOMO and LUMO energy levels are −5.36 and −1.95 eV, respectively, and the calculated first excited state, mainly consisting of a HOMO→LUMO transition, has an excitation energy of 2.86 eV (434 nm) with a small oscillator strength of 0.0972. The incorporation of the electron-donating Ph_2N group onto this skeleton as the *p*-substituent (namely, **1**) results in a significant increase in the HOMO energy level by 0.72 eV, whereas the LUMO level remains almost unchanged. Consequently, the calculated first excited energy of **1** is significantly lowered to 2.28 eV (545 nm). Notably, the HOMO of **1** spreads over the entire π-conjugated skeleton, including the Ph_2N moiety. This change leads to a significant increase in the oscillator strength of the first excited state ($f=0.574$). On the other hand, the introduction of the electron-withdrawing CN group onto the skeleton of **4** (namely, **6**) results in the significant decreases both in the HOMO and LUMO levels by 0.48 and 0.68 eV, respectively. In conjunction with these changes, more importantly, the LUMO of **6** spreads over the entire framework and, consequently, the oscillator strength of the first excited state again increases to 0.552, although its excitation energy (2.81 eV, 442 nm) is comparable to that of **4**. Whereas the accuracy of the calculated excitation energy is not sufficiently high by this level of calculations, the trend in the order of the oscillator strength is in good agreement with the order of the experimentally obtained molecular absorption coefficients for these three molecules. These calculations suggest that the nature of the transition significantly depends on the terminal *p*-substituents. Thus, while the transition in the Ph_2N-substituted **1** has a strong intramolecular CT character, the transition in **6** seems to have a mixed character of the intramolecular CT with the π–π* transition.

Table 4. Photophysical properties of boryl-substituted bis(arylethynyl)-benzenes **1–6** in the spin-coated films.[a]

	λ_{abs} [nm][b]	λ_{em} [nm][c]	Φ_F[d]	τ [ns][e]	$\Delta\lambda$ [cm^{-1}][f]
1	447	562	0.90	1.3/6.9 (37/63)[e]	4580
2	412	508	0.82	2.3/8.8 (55/45)[e]	4590
3	401[g]	486	0.62	2.5/6.5 (57/43)[e]	3700
4	400[g]	476	0.43	1.8/5.7 (73/27)[e]	3990
5	374[g]	459	0.11	0.69/2.5 (84/16)[e]	4950
6	380[g]	462	0.09	0.54/2.0 (88/12)[e]	4670

[a] Spin-coated films were prepared from ca. 1.0 mg mL^{-1} THF solutions. [b] Only the longest absorption maximum wavelengths are given. [c] Fluorescence maximum wavelength, excited at the longest absorption maximum. [d] Absolute quantum yield determined by a calibrated integrating sphere system. [e] Amplitudes of two lifetimes given in parentheses. [f] Stokes shift. [g] Observed as a shoulder band.

Solid-state fluorescence properties: We next investigated the effects of the *p*-substituents on the solid-state fluorescence properties. Thin films of compounds **1–6** were prepared from their THF solutions with ca. 1 mg mL^{-1} concentration on a quartz plate, and their absorption and fluorescence spectra were directly measured. The absolute fluorescence quantum yields were determined by a calibrated integrated sphere system (Hamamatsu C9920). The data are summarized in Table 4.

Both in the absorption and fluorescence spectra, all the compounds **1–6** maintain almost the same spectra as those in benzene solutions, in terms of the maximum wavelengths as well as the full width at the half maximum (FWHM). These results suggest the formation of neither aggregation in the ground state nor an excimer in the excited state. The lateral boryl groups are bulky enough to prevent the intermolecular interaction. It is worth noting that, in all the compounds, the fluorescence quantum yields do not significantly decrease on going from the solution to the solid state. Consequently, a linear relationship is again obtained between the Φ_F and σ_p^+ values in the solid state, as shown in Figure 8, which affords Equation (8). Although a similar linear relationship between the Φ_F and σ_p values has been reported for other oligo(phenyleneethynylene) derivatives in solution,[24] such a relationship in a solid-state emission is unprecedented to the best of our knowledge. In a comparison of Equations (3) and (8), the higher intercept value with the smaller slope constant in Equation (8) demonstrates a trend that the value for Φ_F in the solid state becomes higher than those in solution. This is a notable common feature of the present laterally boryl-substituted bis(arylethynyl)benzene systems, irrespective of the nature of the *p*-substituents at the terminal benzene rings. As far as the molecules have a sufficiently large Stokes shift (>3700 cm^{-1}), the steric bulkiness of the central diborylphenylene core seems sufficient to retain the inherent fluorescence properties even in the solid state, without fluorescence quenching. The increased solid-state Φ_F values observed for compounds **2–6** compared to those in solution may be related to the restricted motion of the molecules in the solid state.[25]

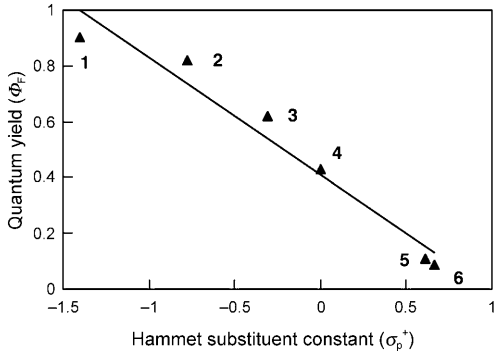

Figure 8. Correlation between the fluorescence quantum yield (Φ_F) in the spin-coated film and the Hammett σ_p^+ constant of the terminal substituents in the boryl-substituted bis(arylethynyl)benzenes **1–6**.

$$\Phi_F = -0.422\sigma_p^+ + 0.409 \quad (r = 0.977) \tag{8}$$

To accumulate more data on the excited-state behavior in the solid state, we determined the fluorescence lifetime of their spin-coated films by a time-resolved photoluminescence study. All the compounds **1–6** showed biexponential decays in the solid state and gave two components, as listed in Table 4. There is a trend in the amplitudes of the two components. Thus, as the *p*-substituent becomes more electron-donating, the longer-lived excited state becomes dominant. However, this trend seems to not be directly related to the increment in the Φ_F value in the solid state compared to that in solution, because all the compounds **1–6** showed comparable or increased solid-state quantum yields, irrespective of the *p*-substituents. According to the time-resolved fluorescence spectra of **4** in the periods of 0–1 and of 3–10 ns right after the excitation, no significant difference in the spectra shape was observed (see the Supporting Information). The characterization of these two components remains unclear at this moment.

Fluorescent sensing of fluoride ions: Because the fluoride ion is highly relevant to human health and environmental issues,[26] the selective detection of it has attracted great attention. Fluorescence sensing is one of the most powerful methods due to its high sensitivity. Tri-coordinate boron compounds are one of the effective fluoride sensors based on the principle that coordination with fluoride ion disrupts the p_π–π^* conjugation between the boron center and the attached π-conjugated chromophore and thus leads to a significant change in the UV/Vis absorption, fluorescence, and two-photon excited fluorescence.[10–15] Considering the characteristic intramolecular CT emission of the present laterally boryl-substituted π systems, we envisioned that the coordination of a fluoride ion to the boron center would interrupt the strong intramolecular CT transition and activate the emission based on the π–π* transition of the bis(arylethynyl)benzene framework, leading to a significant change in the fluorescence spectra. On the basis of this idea, we investigated the fluoride sensing ability of the most emissive **1** as a representative compound for the present borylated π systems.

The titration experiment of **1** with the fluoride ion was carried out in THF by using nBu$_4$NF (TBAF) as the fluoride source. The fluorescence spectral change of **1** (1.96×10^{-6} M) upon the addition of TBAF is shown in Figure 9. A two-step stepwise sensing of the fluoride ions was observed. Thus, as the concentration of TBAF increased, the emission band at 601 nm decreased, and a new blue-shifted band appeared at 477 nm with an isosbestic point at 566 nm (Figure 9a) This change became saturated when the concentration of TBAF amounted to 5.52×10^{-6} M. This spectral change was associated with a dramatic emission color change from reddish orange to greenish blue. The molar ratio analysis showed that the spectral change in this concentration range was attributed to the formation of a 1:1 complex (see the Supporting Information). The binding constant was determined to be $1.25\times10^{5}\,M^{-1}$ at 20 °C, which is comparable to those of other tri-coordinate organoboron compounds.[10–15] Significantly, the further addition of a large excess of TBAF caused the appearance of a more blue-shifted emission band at 412 nm with a new isosbestic point at 460 nm (Figure 9b). This spectral change resulted in an emission color change to bright sky blue. This change can be interpreted as a complexation with a second fluoride ion, and the binding constant was determined to be $1.79\times10^{4}\,M^{-1}$ at 20 °C. Notably, the complexation with fluoride ions did not cause any decrease in the Φ_F value (**1**: 0.61; **1**·F_2^{2-}: 0.76). These high fluorescence efficiencies demonstrate the advantages of our system over the precedent boron-based fluoride ion sensors.

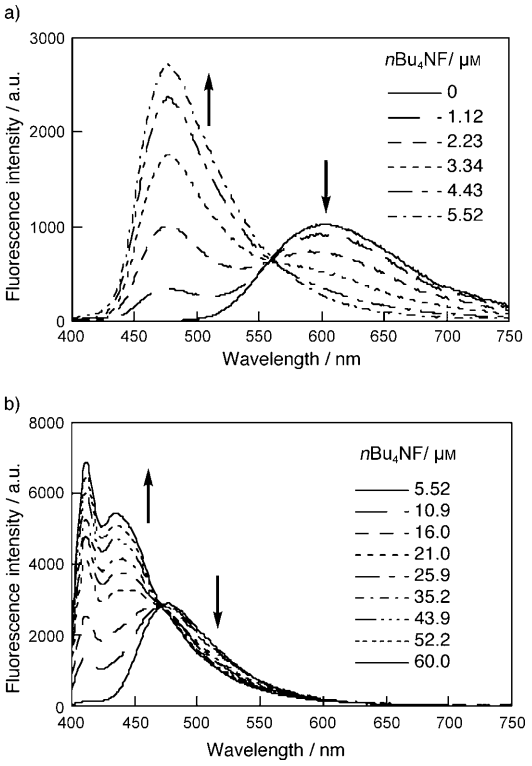

Figure 9. Fluoride ion sensing by Ph_2N-substituted bis(arylethynyl)benzene **1**: Fluorescence spectra change of **1** in THF upon addition of TBAF with the range of a) $0–5.52\times10^{-6}$ M and b) $5.52\times10^{-6}–60.0\times10^{-6}$ M (λ_{ex} = 390 nm).

Conclusions

The introduction of the bulky dimesitylboryl groups onto the lateral positions of the electron-donating π-conjugated systems is an effective design for highly emissive organic solids. We demonstrated the utility and generality of this new design by synthesizing two series of compounds, 2,5-diborylphenylene-cored oligo(phenyleneethynylene) systems and 3-boryl-2,2′-bithiophene systems. In this article, we focused our attention on the former class of compounds and investigated the more detailed structure–property relationships. Thus, we synthesized a series of 1,4-bis(arylethynyl)-2,5-diborylbenzenes **1–6** that contain various *p*-substituents on the terminal benzene rings and investigated the substitu-

ent effects on their absorption and fluorescence properties. Linear relationships were obtained not only between the Hammett σ_p^+ constants of the *p*-substituents and the absorption and fluorescence properties in solutions, but also between the σ_p^+ constants and the fluorescence quantum yields in the solid state. In addition, most of the synthesized derivatives showed enhanced fluorescence in the solid state compared to solution. These findings imply that the present diborylphenylene unit is a very effective and useful core skeleton to prevent fluorescence quenching in the solid state, irrespective of the character of π-conjugated skeletons (namely, electron-donating or -accepting). We also investigated the fluorescence fluoride ion sensing ability of the most emissive **1** and demonstrated the intense fluorescence properties irrespective of the binding modes. This is an important and advantageous feature of the present system over the precedent boron-based fluoride sensors. We believe that our current results would provide an important basis for the further rational design not only of highly emissive organic materials, but also of new boron-based π-conjugated functional materials.

Experimental Section

General procedure: Melting points were measured on a Yanaco MP-S3 instrument. ^{1}H and ^{13}C NMR spectra were recorded with a JEOL A-400 spectrometer (400 MHz for ^{1}H, 100 MHz for ^{13}C NMR). UV/Vis absorption spectra and fluorescence spectra measurements were performed at room temperature with a Shimadzu UV-3150 spectrometer and a Hitachi F-4500 spectrometer, respectively, in degassed spectral grade solvents. Quantum yields were determined with a Hamamatsu C9920–01 calibrated integrating sphere system. TLC was performed on plates coated with 0.25 mm thick silica gel 60F-254 (Merck). Column chromatography was performed by using PSQ 60B (Fuji Silysia). All experiments were carried out under an argon atmosphere.

Computational methods: All calculations were conducted by using the Gaussian 98 program.[27]

1,4-Bis(dimesitylboryl)-2,5-bis(4-methoxyphenylethynyl)benzene (2): (*i*Pr)$_2$NH/THF 1:3 (4 mL) degassed mixed solvent was added to a mixture of **9** (62 mg, 0.1 mmol), 4-iodoanisole (70 mg, 0.3 mmol), [Pd(PPh$_3$)$_4$] (11.6 mg, 0.01 mmol), and CuI (3.9 mg, 0.02 mmol) at room temperature under a stream of argon. The reaction mixture was stirred at 50 °C for 12 h. The solvents were removed under reduced pressure. After addition of $CHCl_3$, the mixture was washed successively with a 5% NH_4OH aqueous solution, 1 N HCl aqueous solution, and brine. The organic layer was dried over anhydrous $MgSO_4$, filtered, and concentrated. The resulting mixture was subjected to silica-gel column chromatography (hexane/$CHCl_3$ 2:1, R_f = 0.32) to afford 44 mg (0.053 mmol) of **2** in 53% yield as a green solid. M.p. > 300 °C; ^{1}H NMR ($CDCl_3$): δ = 7.42 (s, 2H), 6.91 (d, J = 8.4 Hz, 4H), 6.76 (s, 8H), 6.68 (d, J = 8.4 Hz, 4H), 3.78 (s, 6H), 2.26 (s, 12H), 2.03 ppm (s, 24H); ^{13}C NMR ($CDCl_3$): δ = 159.3, 152.0, 142.6, 140.9, 139.1, 137.4, 133.0, 128.4, 125.9, 115.4, 113.4, 93.7, 89.1, 55.2, 23.3, 21.2 ppm; HRMS (FAB): *m*/*z*: calcd for $C_{60}H_{60}B_2O_2$: 834.4779; found: 834.4766.

1,4-Bis(dimesitylboryl)-2,5-bis(4-methylphenylethynyl)benzene (3): This compound was prepared essentially in the same manner as described for **2** by using **9** (93 mg, 0.15 mmol), 4-iodotoluene (98 mg, 0.45 mmol), [Pd(PPh$_3$)$_4$] (17 mg, 0.015 mmol), and CuI (5.7 mg, 0.03 mmol) in (*i*Pr)$_2$NEt/THF 1:3 (6 mL) at 50 °C. Purification by silica-gel column chromatography (hexane/$CHCl_3$ 10:1, R_f = 0.18) afforded 53 mg (0.066 mmol) of **3** in 44% yield as a green solid. M.p. > 300 °C; ^{1}H NMR ($CDCl_3$): δ = 7.48 (s, 2H), 6.99 (d, J = 8.1 Hz, 4H), 6.91 (d, J = 8.1 Hz, 4H), 6.79 (s, 8H), 2.32 (s, 6H), 2.29 (s, 12H), 2.08 ppm (s, 24H); ^{13}C NMR ($CDCl_3$): δ = 152.1, 142.5, 140.9, 139.2, 137.9, 137.4, 131.5, 128.5, 128.4, 125.9, 120.1, 93.9, 89.6, 23.3, 21.4, 21.2 ppm; *m*/*z*: calcd for $C_{60}H_{60}B_2$: 802.4881; found: 802.4879.

1,4-Bis(4-trifluoromethylphenylethynyl)-2,5-bis(dimesitylboryl)benzene (5): This compound was prepared essentially in the same manner as described for **2** by using **9** (62 mg, 0.1 mmol), 4-trifluoromethyl-1-iodobenzene (82 mg, 0.3 mmol), [Pd(PPh$_3$)$_4$] (11.6 mg, 0.01 mmol), and CuI (3.8 mg, 0.02 mmol) in (*i*Pr)$_2$NEt/THF 1:3 (4 mL) at 50 °C. The purification by silica-gel column chromatography (hexane/$CHCl_3$ 5:1, R_f = 0.30) afforded 76 mg (0.083 mmol) of **5** in 84% yield as a pale-yellow solid. M.p. 291–292 °C; ^{1}H NMR ($CDCl_3$): δ = 7.50 (s, 2H), 7.42 (d, J = 8.0 Hz, 4H), 7.07 (d, J = 8.0 Hz, 4H), 6.77 (s, 8H), 2.26 (s, 12H), 2.04 ppm (s, 24H); ^{13}C NMR ($CDCl_3$): δ = 152.4, 142.3, 140.9, 139.5, 137.8, 131.7, 129.1 (q, J = 31 Hz), 128.5, 126.9, 125.7, 124.6 (q, J = 3.3 Hz), 119.9 (q, J = 270 Hz), 92.6, 92.3, 23.3, 21.2 ppm; HRMS (FAB): *m*/*z*: calcd for $C_{64}H_{54}B_2F_6$: 910.4316; found: 910.4312.

1,4-Bis(4-cyanophenylethynyl)-2,5-bis(dimesitylboryl)benzene (6): This compound was prepared essentially in the same manner as described for **2** by using **9** (124 mg, 0.2 mmol), 4-iodobenzonitrile (183 mg, 0.8 mmol), [Pd(PPh$_3$)$_4$] (11.6 mg, 0.01 mmol), and CuI (3.9 mg, 0.02 mmol) in (*i*Pr)$_2$NEt/THF 1:3 (8 mL) at 50 °C. Purification by silica-gel column chromatography (hexane/$CHCl_3$ 5:1, R_f = 0.30) afforded 153 mg (0.186 mmol) of **6** in 93% yield as a pale-yellow solid. M.p. > 300 °C; ^{1}H NMR ($CDCl_3$): δ = 7.53 (s, 2H), 7.47 (d, J = 8.4 Hz, 4H), 7.06 (d, J = 8.4 Hz, 4H), 6.79 (s, 8H), 2.28 (s, 12H), 2.05 ppm (s, 24H); ^{13}C NMR ($CDCl_3$): δ = 152.4, 142.2, 140.9, 139.6, 137.8, 131.9, 131.4, 128.5, 127.9, 125.6, 118.5, 111.1, 94.1, 92.4, 23.3, 21.2 ppm; HRMS (FAB): *m*/*z*: calcd for $C_{60}H_{54}B_2N_2$: 824.4473; found: 824.4475 $[M]^+$..

X-ray crystal structure analysis of compound 4:[28] Single crystals of **4** suitable for X-ray crystal analysis were obtained by recrystallization from CH_2Cl_2/hexane. Intensity data were collected at 173 K on a Rigaku Single Crystal CCD X-ray diffractometer (Saturn 70 with MicroMax-007) with $Mo_{K\alpha}$ radiation (λ = 0.71070 Å) and graphite monochromater. A total of 15390 reflections were measured at a maximum 2θ angle of 50.0°, of which 4092 were independent reflections (R_{int} = 0.0386). The structure was solved by direct methods (SHELXS-97)[29] and refined by the full-matrix least-squares on F^2 (SHELEXL-97).[29] All the non-hydrogen atoms were refined anistropically and all hydrogen atoms were placed by using AFIX instructions. The crystal data are as follows: $C_{58}H_{56}B_2$; F_W = 774.65; crystal size = 0.20 × 0.20 × 0.20 mm^3; monoclinic; $P2_1/a$; a = 11.285(3), b = 16.755(2), c = 12.332(3) Å; β = 93.3667(14)°; V = 2327.7(10) Å^3; Z = 2; ρ_{calcd} = 1.105 g cm^{-3}. The refinement converged to R_1 = 0.0572, wR_2 = 0.1433 ($I > 2\sigma(I)$); GOF = 1.084.

X-ray crystal structure analysis of compound 6:[28] Single crystals of **6** suitable for X-ray crystal analysis were obtained by recrystallization from CH_2Cl_2/hexane. Intensity data were collected at 173 K on a Rigaku Single Crystal CCD X-ray diffractometer (Saturn 70 with MicroMax-007) with $Mo_{K\alpha}$ radiation (λ = 0.71070 Å) and a graphite monochromater. A total of 15383 reflections were measured at a maximum 2θ angle of 50.0°, of which 4143 were independent reflections (R_{int} = 0.0558). The structure was solved by direct methods (SHELXS-97)[29] and refined by the full-matrix least-squares on F^2 (SHELEXL-97).[29] All the non-hydrogen atoms were refined anistropically and all hydrogen atoms were placed by using AFIX instructions. The crystal data are as follows: $C_{60}H_{54}B_2N_2$; F_W = 824.67; crystal size = 0.20 × 0.15 × 0.05 mm^3; monoclinic; $P2_1/n$; a = 12.418(3), b = 8.274(2), c = 22.965(6) Å; β = 90.0707(16)°, V = 2359.5 (11) Å^3; Z = 2; ρ_{calcd} = 1.161 g cm^{-3}. The refinement converged to R_1 = 0.0709, wR_2 = 0.1492 ($I > 2\sigma(I)$); GOF = 1.149.

Acknowledgements

This work was partly supported by Grants-in-Aid (no. 19675001 and 17069011) from the Ministry of Education, Culture, Sports, Science, and Technology (Japan).

[1] For reviews, see: a) C. D. Entwistle, T. B. Marder, *Angew. Chem.* **2002**, *114*, 3051–3056; *Angew. Chem. Int. Ed.* **2002**, *41*, 2927–2931; b) C. D. Entwistle, T. B. Marder, *Chem. Mater.* **2004**, *16*, 4574–4585; c) "Boron: Organoboranes": F. Jäkle in *Encyclopedia of Inorganic Chemistry*, 2nd ed. (Ed.: R. B. King), Wiley, New York, **2005**; d) F. Jakle, *Coord. Chem. Rev.* **2006**, *250*, 1107–1121; e) S. Yamaguchi, A. Wakamiya, *Pure Appl. Chem.* **2006**, *78*, 1413–1424.

[2] a) Z. Yuan, N. J. Taylor, T. B. Marder, I. D. Williams, S. K. Kurtz, L.-T. Cheng, *J. Chem. Soc. Chem. Commun.* **1990**, 1489–1492; b) Z. Yuan, N. J. Taylor, Y. Sun, T. B. Marder, I. D. Williams, L.-T. Cheng, *J. Organomet. Chem.* **1993**, *449*, 27–37; c) Z. Yuan, N. J. Taylor, R. Ramachandran, T. B. Marder, *Appl. Organomet. Chem.* **1996**, *10*, 305–316; d) Z. Yuan, J. C. Collings, N. J. Taylor, T. B. Marder, C. Jardin, J.-F. Halet, *J. Solid State Chem.* **2000**, *154*, 5–12; e) Z. Yuan, C. D. Entwistle, J. C. Collings, D. Albesa-Jové, A. S. Batsanov, J. A. K. Howard, N. J. Taylor, H. M. Kaiser, D. E. Kaufmann, S.-Y. Poon, W.-Y. Wong, C. Jardin, S. Fathallah, A. Boucekkine, J.-F. Halet, T. B. Marder, *Chem. Eur. J.* **2006**, *12*, 2758–2771.

[3] a) M. Lequan, R. M. Lequan, C. K. Ching, *J. Mater. Chem.* **1991**, *1*, 997–999; b) C. Branger, M. Lequan, R. M. Lequan, M. Barzoukas, A. Fort, *J. Mater. Chem.* **1996**, *6*, 555–558; c) C. Branger, M. Lequan, R. M. Lequan, M. Large, F. Kajzar, *Chem. Phys. Lett.* **1997**, *272*, 265–270.

[4] a) Z.-Q. Liu, Q. Fang, D. Wang, G. Xue, W.-T. Yu, Z.-S. Shao, M.-H. Jiang, *Chem. Commun.* **2002**, 2900–2901; b) D. X. Cao, Z. Q. Liu, Q. Fang, G. B. Xu, G. Xue, G. Q. Liu, W. T. Yu, *J. Organomet. Chem.* **2004**, *689*, 2201; c) Z.-Q. Liu, Q. Fang, D.-X. Cao, D. Wang, G.-B. Xu, *Org. Lett.* **2004**, *6*, 2933–2936.

[5] J. C. Collings, S.-Y. Poon, C. L. Droumaguet, M. Charlot, C. Katan, L.-O. Pålsson, A. Beedy, J. A. Mosely, H. M. Kaiser, D. Kaufmann, W.-Y. Wong, M. Blanchard-Desce, T. B. Marder, *Chem. Eur. J.* **2009**, *15*, 198–208.

[6] a) T. Noda, Y. Shirota, *J. Am. Chem. Soc.* **1998**, *120*, 9714–9715; b) T. Noda, H. Ogawa, Y. Shirota, *Adv. Mater.* **1999**, *11*, 283–285; c) Y. Shirota, M. Kinoshita, T. Noda, K. Okumoto, T, Ohara, *J. Am. Chem. Soc.* **2000**, *122*, 11021–11022; d) T. Noda, Y. Shirota, *J. Lumin.* **2000**, *87*, 1168–1170; e) H. Kinoshita, H. Kita, Y. Shirota, *Adv. Funct. Mater.* **2002**, *12*, 780–786; f) H. Doi, M. Kinoshita, K. Okumoto, Y. Shirota, *Chem. Mater.* **2003**, *15*, 1080–1089.

[7] a) W.-L. Jia, D. Song, S. Wang, *J. Org. Chem.* **2003**, *68*, 701–705; b) W.-L. Jia, D.-R. Bai, T. McCormick, Q.-D. Liu, M. Motala, R.-Y. Wang, C. Seward, Y. Tao, S. Wang, *Chem. Eur. J.* **2004**, *10*, 994–1006; c) W. L. Jia, M. J. Moran, Y. Y. Yuan, Z. H. Lu, S. Wang, *J. Mater. Chem.* **2005**, *15*, 3326–3333; d) W. L. Jia, X. D. Feng, D. R. Bai, Z. H. Lu, S. Wang, G. Vamvounis, *Chem. Mater.* **2005**, *17*, 164–170.

[8] M. Mazzeo, V. Vitale, F. D. Sala, M. Anni, G. Barbarella, L. Favaretto, G. Sotgiu, R. Cingolani, G. Gigli, *Adv. Mater.* **2005**, *17*, 34–39.

[9] S.-L. Lin, L.-H. Chan, R.-H. Lee, M.-Y. Yen, W.-J. Kuo, C.-T. Chen, R.-J. Jeng, *Adv. Mater.* **2008**, *20*, 3947–3952.

[10] a) S. Yamaguchi, S. Akiyama, K. Tamao, *J. Am. Chem. Soc.* **2000**, *122*, 6335–6336; b) S. Yamaguchi, S. Akiyama, K. Tamao, *J. Am. Chem. Soc.* **2001**, *123*, 11372–11375; c) S. Yamaguchi, T. Shirasaka, S. Akiyama, K. Tamao, *J. Am. Chem. Soc.* **2002**, *124*, 8816–8817; d) Y. Kubo, M. Yamamoto, M. Ikeda, M. Takeuchi, S. Shinkai, S. Yamaguchi, K. Tamao, *Angew. Chem.* **2003**, *115*, 2082–2086; *Angew. Chem. Int. Ed.* **2003**, *42*, 2036–2040.

[11] a) S. Solé, F. P. Gabbaï, *Chem. Commun.* **2004**, 1284–1285; b) M. Melaimi, F. P. Gabbaï, *J. Am. Chem. Soc.* **2005**, *127*. 9680–9681; c) C.-W. Chiu, F. P. Gabbaï, *J. Am. Chem. Soc.* **2006**, *128*, 14248–14249; d) T. W. Hudnall, M. Melaimi, F. P. Gabbaï, *Org. Lett.* **2006**, *8*, 2747–2749; e) T. W. Hundall, F. P. Gabbaï, *J. Am. Chem. Soc.* **2007**, *129*, 11978–11986; f) M. H. Lee, T. Agou, J. Kobayashi, T. Kawashima, F. P. Gabbaï, *Chem. Commun.* **2007**, 1133–1135.

[12] M. Miyata, Y. Chujo, *Polym. J.* **2002**, *34*, 967–969.

[13] a) A. Sundararaman, M. Victor, R. Varughese, F. Jäkle, *J. Am. Chem. Soc.* **2005**, *127*, 13748–13749; b) A. Sundararaman, K. Venkatasubbaiah, M. Victor, L. N. Zakharov, A. L. Rheingold, F. Jäkle, *J. Am. Chem. Soc.* **2006**, *128*, 16565.

[14] Z.-Q. Liu, M. Shi, F.-U. Li, Q. Fang, Z.-H. Chen, T. Yi, C.-H. Huang, *Org. Lett.* **2005**, *7*, 5481–5484.

[15] a) X. Y. Liu, D. R. Bai, S. Wang, *Angew. Chem.* **2006**, *118*, 5601–5604; *Angew. Chem. Int. Ed.* **2006**, *45*, 5475–5478; b) D. R. Bai, X.-Y. Liu, X. S. Wang, *Chem. Eur. J.* **2007**, *13*, 5713–5723; c) S.-B. Zhao, T. McCormick, S. Wang, *Inorg. Chem.* **2007**, *46*, 10965–10967.

[16] a) C.-H. Zhao, A. Wakamiya, Y. Inukai, S. Yamaguchi, *J. Am. Chem. Soc.* **2006**, *128*, 15934–15935; b) C.-H. Zhao, A. Wakamiya, S. Yamaguchi, *Macromolecules* **2007**, *40*, 3898–3900; c) A. Wakamiya, K. Mori, S. Yamaguchi, *Angew. Chem.* **2007**, *119*, 4351–4354; *Angew. Chem. Int. Ed.* **2007**, *46*, 4273–4276.

[17] H. Li, A. Sundararaman, K. Venkatasubbaiah, F. Jäkle, *J. Am. Chem. Soc.* **2007**, *129*, 5792–5793.

[18] M. Elbing, G. C. Bazan, *Angew. Chem.* **2008**, *120*, 846–850; *Angew. Chem. Int. Ed.* **2008**, *47*, 834–838.

[19] For example, see: a) C.-T. Chen, C.-L. Chiang, Y.-C. Lin, L.-H. Chan, C.-H. Huang, Z.-W. Tsai, C.-T. Chen, *Org. Lett.* **2003**, *5*, 1261–1264; b) H. Langhals, O. Krotz, K. Polborn, P. Mayer, *Angew. Chem.* **2005**, *117*, 2479–2480; *Angew. Chem. Int. Ed.* **2005**, *44*, 2427–2428; c) S. H. Lee, B.-B. Jang, Z. H. Kafafi, *J. Am. Chem. Soc.* **2005**, *127*, 9071–9078; d) Y. Kim, J. Bouffard, S. E. Kooi, T. M. Swager, *J. Am. Chem. Soc.* **2005**, *127*, 13726–13731; e) Z. Xie, B. Yang, F. Li, G. Cheng, L. Liu, G. Yang, H. Xu, L. Ye, M. Hanif, S. Liu, D. Ma, Y. Ma, *J. Am. Chem. Soc.* **2005**, *127*, 14152–14513; f) A. Hayer, V. Halleux, A. Köhler, A. El-Garoughy, E. W. Meijer, J. Barberá, J. Tant, J. Levin, M. Lehmann, J. Gierschner, J. Cornil, Y. H. Geerts, *J. Phys. Chem. A* **2006**, *110*, 7653–7659.

[20] A. Iida, S. Yamaguchi, *Chem. Commun.* **2009**, 3002–3004.

[21] a) L. Blankenburg, E. Klemm, *Des. Monomers Polym.* **2003**, *6*, 57–65; b) S. W. Thomas, T. M. Swager, *Macromolecules* **2005**, *38*, 2716–2718.

[22] "Correlation of Structure with Reactivity": N. S. Isaacs in *Physical Organic Chemistry*, 1st ed., Universities Press, Belfast, **1987**, pp. 129–170.

[23] a) B. Strehmel, A. M. Sarker, J. H. Malpert, V. Strehmel, H. Seifert, D. C. Neckers, *J. Am. Chem. Soc.* **1999**, *121*, 1226–1236; b) F. C. Krebs, H. Spanggaard, *J. Org. Chem.* **2002**, *67*, 7185–7192.

[24] a) Y. Yamaguchi, T. Tanaka, S. Kobayshi, T. Wakamiya, Y. Matsubara, Z. Yoshida, *J. Am. Chem. Soc.* **2005**, *127*, 9332–9333; b) Y. Yamaguchi, T. Ochi, T. Wakamiya, Y. Matsubara, Z. *Yoshida*, *Org. Lett.* **2006**, 8, 717–720.

[25] a) J. Luo, Z. Xie, J. W. Y. Lam, L. Cheng, H. Chen, C. Qiu, H. S. Kwok, X. Zhan, Y. Liu, D. Zhu, B. Z. Tang, *Chem. Commun.* **2001**, 1740–1741; b) H. Tong, Y. Dong, M. Häuβler, J. W. Y. Lam, H. H.-Y. Sung, I. D. Williams, J. Sun, B. Z. Tang, *Chem. Commun.* **2006**, 1133–1135; c) H. Tong, Y. Hong, Y. Dong, M. Häuβler, J. W. Y. Lam, Z. Li, Z. Guo, Z. Guo, B. Z. Tang, *Chem. Commun.* **2006**, 3705–3707.

[26] a) K. Kirk, *Biochemistry of the Halogens and Inorganic Halides*, Plenum Press, New York, **1991**, p. 58; b) A. Wiseman, *Handbook of Experimental Pharmacology XX/2, Part 2*, Springer, Berlin, **1970**, p. 48; c) C. B. Black, B. Andrioletti, A. C. Try, C. Ruiperez, J. L. Sessler, *J. Am. Chem. Soc.* **1999**, *121*, 10438–10439; d) H. Sohn, S. Létant, M. J. Sailor, W. C. Trogler, *J. Am. Chem. Soc.* **2000**, *122*, 5399–5400.

[27] Gaussian 98, Revision A.5, M. J. Frisch, G. W. Trucks, H. B. Schlegel, G. E. Scuseria, M. A. Robb, J. R. Cheeseman, V. G. Zakrzewski, J. A. Montgomery, Jr., R. E. Stratmann, J. C. Burant, S. Dapprich, J. M. Millam, A. D. Daniels, K. N. Kudin, M. C. Strain, O. Farkas, J. Tomasi, V. Barone, M. Cossi, R. Cammi, B. Mennucci, C. Pomelli, C. Adamo, S. Clifford, J. Ochterski, G. A. Petersson, P. Y. Ayala, Q. Cui, K. Morokuma, D. K. Malick, A. D. Rabuck, K. Raghavachari, J. B. Foresman, J. Cioslowski, J. V. Ortiz, B. B. Stefanov, G. Liu, A. Liashenko, P. Piskorz, I. Komaromi, R. Gomperts, R. L. Martin, D. J. Fox, T. Keith, M. A. Al-Laham, C. Y. Peng, A. Nanayakkara, C. Gonzalez, M. Challacombe, P. M. W. Gill, B. G. Johnson, W.

Chen, M. W. Wong, J. L. Andres, M. Head-Gordon, E. S. Replogle, J. A. Pople, Gaussian, Inc., Pittsburgh, PA, **1998**.

[28] Crystal data for **4** and **6**: see the Supporting Information. CCDC-709030 (**4**) and 709031 (**6**) contain the supplementary crystallographic data for this paper. These data can be obtained free of charge from The Cambridge Crystallographic Data Centre via www.ccdc.cam.ac.uk/data_request/cif.

[29] SHELX-97, Program for the Refinement of Crystal Structure, G. M. Sheldrick, University of Göttingen, Göttingen (Germany), **1997**.

Received: April 2, 2009
Published online: September 8, 2009

